

## LONG-WAVELENGTH TOPOGRAPHIC CHANGE ON MERCURY: EVIDENCE AND MECHANISMS.

Sean C. Solomon<sup>1</sup>, Christian Klimczak<sup>1</sup>, Paul K. Byrne<sup>1</sup>, Steven A. Hauck, II<sup>2</sup>, Jeffrey A. Balcerski<sup>2</sup>, Andrew J. Dombard<sup>3</sup>, Maria T. Zuber<sup>4</sup>, David E. Smith<sup>4</sup>, Roger J. Phillips<sup>5</sup>, James W. Head<sup>6</sup>, and Thomas R. Watters<sup>7</sup>.

<sup>1</sup>Department of Terrestrial Magnetism, Carnegie Institution of Washington, Washington, DC 20015, USA (scs@dtm.ciw.edu); <sup>2</sup>Dept. of Earth, Environmental and Planetary Sciences, Case Western Reserve University, Cleveland, OH 44106, USA; <sup>3</sup>Dept. of Earth and Environmental Sciences, University of Illinois at Chicago, Chicago, IL 60607, USA; <sup>4</sup>Dept. of Earth, Atmospheric, and Planetary Sciences, Massachusetts Institute of Technology, Cambridge, MA 02139, USA; <sup>5</sup>Planetary Science Directorate, Southwest Research Institute, Boulder, CO 80302; <sup>6</sup>Department of Geological Sciences, Brown University, Providence, RI 02912, USA; <sup>7</sup>Center for Earth and Planetary Studies, National Air and Space Museum, Smithsonian Institution, Washington, DC 20560, USA.

**Introduction:** The Mercury Surface, Space ENvironment, GEOchemistry, and Ranging (MESSENGER) spacecraft, in orbit about Mercury since March 2011, has been accumulating evidence that Mercury experienced changes in long-wavelength topography more recently than the end of late heavy bombardment and the volcanic emplacement of the largest expanses of smooth plains. That evidence comes from measurements with MESSENGER's Mercury Laser Altimeter (MLA) [1], a recent determination of Mercury's gravity field [2], and a variety of analyses conducted with images obtained by MESSENGER's Mercury Dual Imaging System (MDIS) [3-6]. Here we summarize key example observations, and we discuss several possible mechanisms for such long-wavelength changes, all tied to the thermal evolution of Mercury's interior [e.g., 7].

**Caloris basin:** MLA altimetry [1] has confirmed earlier results from stereo analysis of flyby images [3] that the smooth plains interior to the Caloris impact basin display long-wavelength variations in topography that appear not to be the result of volcanic construction during plains emplacement. The magnitude of these variations, up to ~3 km, is such that portions of the northern floor stand higher than the basin rim [1,3]. The elevated portion of the northern Caloris floor appears to be part of a quasi-linear rise that trends generally west-southwest–east-northeast and extends over approximately half the circumference of Mercury at mid-latitudes. The floors of younger impact craters within and near Caloris tilt in directions that generally correlate with the long-wavelength topography of the region [1,6] and are consistent with modification of Mercury's long-wavelength topography after both the formation of the Caloris basin and the emplacement of its interior and exterior volcanic plains somewhat more recently than 3.8 Ga [8,9].

**Northern rise:** Within Mercury's northern smooth plains [10] is a broad area ~1,000 km across that rises ~1.5 km above the surrounding terrain (Fig. 1). Much of the boundary of the northern plains follows a gravitational equipotential [2], and there is strong geological [10] and geochemical [11] evidence that the lavas that

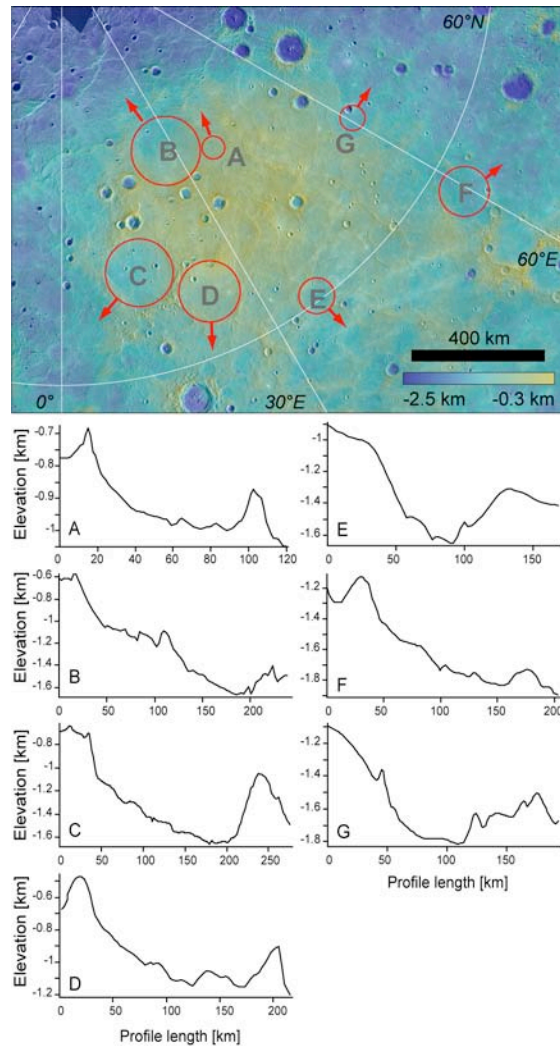


**Figure 1.** (Top) Map of northern rise showing volcanically flooded impact craters with floors that tilt away from the locus of highest elevation (gridded MLA topography overlaid on MDIS global mosaic). (Bottom) Elevation profiles across the craters labeled at top. From [4].

formed the plains were highly fluid. The surface of the rise is indistinguishable from that of the surrounding plains with respect to morphology [10] and kilometer-scale slopes [1], and the rise is marked by a positive

free-air gravity anomaly consistent with little contrast in crustal thickness from the adjacent plains [2]. Emplacement of the northern plains resulted in the flooding of many impact craters and basins [10], and the floors of flooded craters on the northern rise tilt away from the center of the rise (Fig. 1) at angles that agree well with the large-scale slope of rise topography. Uplift of the northern rise at a time following plains emplacement is strongly indicated by these observations.

**Lava channels:** Near the northern plains are several channels that cut through the surrounding inter-crater terrain and closely resemble surface flow features observed on Earth and Mars [5,10]. The channels display braided textures and elongate, tapered “islands,” features characteristic of erosion by the above-ground movement of a low-viscosity fluid and from which the flow direction may be inferred. Topographic profiles, however, indicate that several such channels are not consistently downhill in the direction of original flow (Fig. 2). Although a constructional component to relief cannot be discounted at the shortest scales, the modern topographic profiles suggest that at the scales of several hundred kilometers the topography has been modified since channel formation.

**Tectonic systems bounding high terrain:** The combination of MDIS global image mosaics and MLA northern-hemisphere topography has revealed that a number of areas of high-standing terrain on Mercury are bordered by fold-and-thrust belts that extend for hundreds of kilometers or more [12]. On the basis of both morphology and crater transection relations, these tectonic belts were active well after the end of heavy bombardment. Tilt directions of crater floors near these boundaries suggest that continued slip on the fault systems contributed additional topographic relief [12].

**Possible mechanisms:** The growing evidence for widespread changes in long-wavelength topography on Mercury since 3.8 Ga points to a global mechanism for most such changes. Two candidate processes are mantle dynamic stresses and accommodation of global contraction. Some models of mantle convection on Mercury are permissive of dynamic topography of sufficient magnitude and horizontal wavelength to account for at least a subset of observations [13], but other models predict much less surface topographic change than has been documented [13,14]. Moreover, the question of whether mantle convection operates today is open [14]. The fold-and-thrust belts bounding some areas of high terrain on Mercury favor a contribution to topographic change from global contraction, but not all areas of topographic change display bounding fault systems. An alternative mechanism for global contraction is lithospheric folding [15]. Folding models

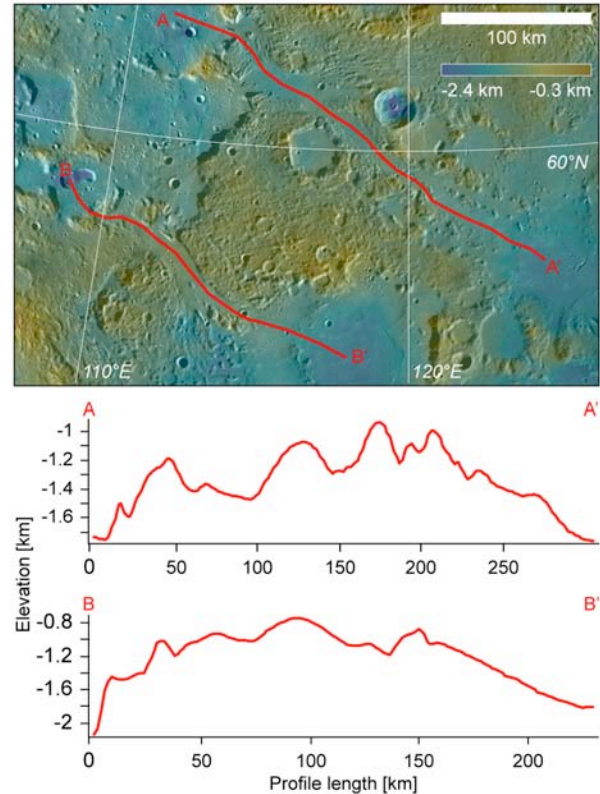


**Figure 2.** (Top) Map view of two lava channels near the northern rise (gridded MLA topography overlaid on MDIS global mosaic). (Bottom) Elevation profiles along the two channels. From [5].

(in Cartesian geometry) are consistent with observed horizontal wavelengths of topographic change for a subset of possible interior thermal structures [15].

**Conclusions:** Mercury experienced widespread changes in long-wavelength topography since 3.8 Ga. Further analysis of specific examples and the development of new models for candidate processes should provide new constraints on global cooling and the accumulated global contraction [7] during that time.

**References:** [1] M. T. Zuber et al. (2012) *Science*, submitted. [2] D. E. Smith et al. (2012) *Science*, submitted. [3] J. Oberst et al. (2010) *Icarus* 209, 230. [4] C. Klimczak et al. (2012) *JGR*, submitted. [5] P. K. Byrne et al. (2012) *JGR*, submitted. [6] J. A. Balcorski et al. (2012), *LPS* 43, this mtg. [7] S. A. Hauck, II, et al. (2004) *EPSL* 222, 713. [8] R. G. Strom et al. (2008) *Science* 321, 79. [9] C. I. Fassett et al. (2009) *EPSL* 285, 297. [10] J. W. Head et al. (2011) *Science* 333, 1853. [11] L. R. Nittler et al. (2011) *Science* 333, 1847. [12] P. K. Byrne et al. (2012) *LPS* 43, this mtg. [13] S. D. King (2008) *Nature Geosci.* 1, 229. [14] N. C. Michel (2012) *LPS* 43, this mtg. [15] A. J. Dombard et al. (2001) *LPS* 32, 2035.